



Expression patterns of two heat-shock cognate 70 genes during immune responses and larval development of the Chinese mitten crab *Eriocheir sinensis*

P. Li, X.F. Jiang, W.B. Guo, J. Yan and K.Y. Zhou

Jiangsu Key Laboratory for Biodiversity and Biotechnology and Jiangsu Key Laboratory for Aquatic Crustacean Diseases, College of Life Sciences, Nanjing Normal University, Nanjing, Jiangsu, China

Corresponding authors: P. Li / K.Y. Zhou
E-mail: biolipeng@163.com / kyzhounj@126.com

Genet. Mol. Res. 15 (3): gmr.15036319
Received March 23, 2016
Accepted May 25, 2016
Published September 16, 2016
DOI <http://dx.doi.org/10.4238/gmr.15036319>

Copyright © 2016 The Authors. This is an open-access article distributed under the terms of the Creative Commons Attribution ShareAlike (CC BY-SA) 4.0 License.

ABSTRACT. Two heat-shock protein (HSP) 70 family transcripts, heat-shock protein 70 cognate 5 and heat-shock protein 70 cognate 3 (designated as *EsHSC70-5* and *EsHSC70-3*, respectively), were isolated from the Chinese mitten crab *Eriocheir sinensis* and their expression profiles were evaluated for their responsiveness to larval development and immune challenge in adult crabs. The HSPs exhibited 45-89% identity with other heat-shock proteins, and they shared similar structural features. *EsHSC70* mRNA expression was detected not only during infection but also during the developmental larval stages. The *EsHSC70s* were enriched, and their expression fluctuated during early development. *EsHSC70* mRNA expression was significantly induced by *Vibrio parahaemolyticus* challenge in all of the tissues studied ($P <$

0.05). Expression of *EsHSC70* mRNA in the hepatopancreas and at the early zoeal stages was particularly pronounced, and the two *EsHSC70s* exhibited differential expression patterns both chronologically and spatially. The *EsHSC70-5* mRNA level was significantly downregulated in the intestine and gills compared to that in controls at nearly all time points, and was expressed at a lower level after the bacterial challenge, indicating that *EsHSC70-5* and *EsHSC70-3* respond to immune challenges. The stage-specific enrichment of *EsHSC70* transcripts in crabs suggests that these stress proteins play an essential role during brachyurization events.

Key words: *Eriocheir sinensis*; Heat-shock cognate protein 70; mRNA expression; Brachyurization development; Immune challenge

INTRODUCTION

Heat-shock proteins (HSPs) are a family of ubiquitously expressed proteins that are conserved in many different kinds of organisms. HSPs are divided into several families according to their molecular weights, homologies, and functions, and include HSP110, HSP100, HSP90, HSP70, HSP60, HSP40, and small HSPs (sHSPs, with molecular weights ranging from 12 to 42 kDa) (Wang et al., 2013). The eukaryotic HSP70 family consists of four monophyletic groups: cytosol, endoplasmic reticulum, mitochondria, and chloroplast HSP70s (Kregel, 2002; Bausero et al., 2005). HSP70s act as molecular chaperones, and their expression is regulated by environmental and physiological stressors (Sun et al., 2012; Chichester et al., 2015) and non-stressful conditions, such as cell growth, development, and pathophysiological conditions (Behnke and Hendershot, 2014; Tiroli-Cepeda et al., 2014). Their functions include translocation, folding newly synthesized proteins, degradation of unstable and misfolded proteins, as well as the prevention and dissolution of protein complexes. Molecular chaperones are probably the only proteins involved in infections that have dual roles as pathogen-associated molecular patterns and pattern recognition receptors (Das et al., 2015). The cognate forms of HSP70, the heat-shock cognate proteins 70 (HSC70s), are abundantly and ubiquitously expressed in all cells, are present under most conditions, and may or may not be influenced by stress (Daugaard et al., 2007; Zhang and Denlinger, 2010). HSC70s function as molecular chaperones or housekeeping proteins, and have been shown to be involved in many cellular physiological processes, such as protein folding in the cytoplasm, cell survival during neurulation, prevention of apoptosis induced by virus infections, and trafficking of receptors and coated vesicles (Guerrero et al., 2002; Yan et al., 2010; Iwanaga et al., 2014). HSC70s also act as molecular chaperones to regulate *MeVg2* expression in the greasyback shrimp (*Metapenaeus ensis*) (Chan et al., 2014). Some HSC70 cDNAs have been isolated, and the expression patterns of these genes have been investigated in several crustaceans, including the giant freshwater prawn *Macrobrachium rosenbergii* (Liu et al., 2004), the oriental river prawn *Macrobrachium nipponense* (Xiu et al., 2014), and the greasyback shrimp (Chan et al., 2014). However, no studies have been conducted on HSC70s in brachyuran decapod crustaceans.

The Gram-negative bacterium *Vibrio parahaemolyticus* is one of the most important pathogens in crab seed breeding and aquaculture (Wan et al., 2000; Xu et al., 2002). It also causes

high mortality in broodstock populations of the Chinese mitten crab (*Eriocheir sinensis*) during reproduction (Cheng et al., 2013). At present, it is still unclear whether heat-shock cognate proteins are involved in metamorphosis and bacterial challenges in the Chinese mitten crab. In the present study, we identified full-length cDNAs of two HSP70 family transcripts: HSP70 cognate 5 and HSP70 cognate 3 (designated as *EsHSC70-5* and *EsHSC70-3*, respectively) from *E. sinensis*, and examined their expression profiles in response to larval brachyurization and *V. parahaemolyticus* challenge in adult crabs. These HSC70 cDNA and mRNA expression data will provide useful molecular information for further investigations of their roles in the development and innate immunity of crabs.

MATERIAL AND METHODS

Experimental animals and sample preparation

Whole-body tissue samples from *E. sinensis* embryos (stage O, embryo stage; heartbeat, 90 times/min) and nine larval stages (stage Z1, the 1st zoeal stage; stage Z2, the 2nd zoeal stage; stage Z3, the 3rd zoeal stage; stage Z4, the 4th zoeal stage; stage Z5, the 5th zoeal stage; stage M, megalopa stage; stage J1, the 1st juvenile crab stage; stage J2, the 2nd juvenile crab stage; stage J3, the 3rd juvenile crab stage) were collected from an aquatic nursery. The samples (each about 15 to 30 mg in weight) were isolated at the 10 stages (Table S1). The samples were dissected and preserved in RNAlater RNA Stabilization Reagent (Qiagen, Germany), cut into tiny particles (less than 0.2 mm thick) in separate tubes, kept overnight at 4°C, and finally stored at -20°C before total RNA isolation.

Adult *E. sinensis* crabs (with an average mass of about 100 g) were collected from an aquaculture farm. The crabs were placed in aerated glass containers that were filled with a circular flow of fresh water at a density of 10 crabs per tank, and were acclimated for more than two weeks before the bacterial infection experiment. *V. parahaemolyticus* (Collector No. 1.1614) was purchased from the China General Microbiological Culture Collection Center. After rejuvenation, the strain was static-cultured in Luria Bertani medium at 28°C for 24 h. The bacteria were then washed off and diluted into 1×10^7 colony-forming units (CFU)/mL in 0.1 M phosphate-buffered saline (PBS, pH 7.4). Live *V. parahaemolyticus* (1.0×10^7 CFU/100 g body weight) were injected into the arthrodial membrane of the last pair of walking legs of 30 crabs that were then placed in clean tanks. Meanwhile, 30 other crabs were injected with PBS (0.1 M/100 g body weight) as controls. Thirty crabs that were fed normally and not injected were used as blank controls. The procedures adopted in this study were approved by the Institutional Animal Care and Use Committee of Nanjing Normal University [SOXR (Jiangsu) 2012-004]. Five crabs were randomly sampled at time intervals of 0, 6, 12, 24, 36, and 48 h after *V. parahaemolyticus* or PBS injection. Various tissue samples (heart, gills, hepatopancreas, and intestine) were collected from the infected and control crabs. The samples were harvested as described above and stored at -20°C before total RNA isolation.

Total RNA isolation and cDNA synthesis

Total RNA from the tissues was extracted separately using an RNeasy® Mini Kit (Qiagen) according to the instruction manual. The quality and quantity of total RNA were determined by agarose gel electrophoresis and absorbance spectrophotometry in a

BioPhotometer (Eppendorf, Germany). The cDNAs used to obtain 5'- and 3'-end sequences of each gene were synthesized using the 5'-RACE System for Rapid Amplification of cDNA Ends (RACE), Version 2.0 (Invitrogen, USA) and the SMART™ RACE cDNA Amplification Kit (Clontech, USA) with SuperScript II RT (Invitrogen), following the manufacturer protocol. The synthesized cDNA was stored at -70°C until use.

Cloning of full-length cDNA sequences using RACE

The full-length cDNA sequences of *EsHSC70-5* and *EsHSC70-3* were made up of 5'-RACE segments, expressed sequence tag (EST) segments, and 3' RACE segments. Based on EST information (412 bp, dbEST_Id 62013203, and GenBank accession No. GE329279 for *HSC70-5*; 255 bp, dbEST_Id 62013204, and GenBank accession No. GE329280 for *HSC70-3*), new gene-specific primers (Table 1) were designed and synthesized to obtain full-length cDNA sequences. The primers used were a 10-μM abridged anchor primer, a 10-μM anchor primer, and a 10-μM abridged universal anchor primer or a 10-μM universal amplification primer. HSC705-GSP51/HSC705-GSP52/HSC705-GSP53 for *EsHSC70-5* and HSC703-GSP1/HSC703-GSP2/HSC703-GSP3 for *EsHSC70-3* were used to amplify the 5'-ends of each cDNA. A 10X Universal Primer A Mix (UPM) and HSC705-GSP31/HSC705-GSP32 for *EsHSC70-5* and a UPM and HSC70-31/HSC70-32 for *EsHSC70-3* were used to obtain the 3'-ends of each cDNA. Polymerase chain reactions (PCRs) with HSC705-QCF/HSC705-QCR and HSC703-QCF/HSC703-QCR were used to amplify the open reading frames (ORFs) of *EsHSC70-5* and *EsHSC70-3* cDNA, respectively. The PCR products were separated on 2% agarose gel, and bands of the expected size were cut from the gel and purified using a gel purification kit (Axygen, USA). The freshly purified PCR products were cloned into a pMD19-T vector (TaKaRa, Japan) and sequenced. The sequences obtained after 5'- and 3'-RACE were assembled using the DNASTar Lasergene 7.1 software to generate full-length cDNA.

EsHSC70-5 and *EsHSC70-3* expression profiles

The mRNA expression profiles of *EsHSC70-5* and *EsHSC70-3* were examined using the real-time fluorescent quantitative PCR (RT-qPCR) method. In addition, a semi-quantitative reverse transcription PCR (SqRT-PCR) was used to investigate *EsTUBA* expression at different developmental stages.

Total RNA was isolated using an RNeasy Mini Kit (Qiagen). cDNA first-strand synthesis was conducted based on PrimeScript™ RT Reagent usage information (TaKaRa), using total RNA treated with DNase I (TaKaRa) as a template. The cDNA mix was diluted to 1:10 with Milli-Q water (Toyobo, Japan), and stored at -20°C until used as a template for subsequent RT-qPCRs and SqRT-PCRs. All of the primers used for RT-qPCR and SqRT-PCR were designed according to the corresponding sequences in *E. sinensis* (Table 1). The gene-specific primers qHSC705-F and qHSC705-R were used to amplify a 106-bp product for *EsHSC70-5*, and the gene-specific primers qHSC703-F and qHSC705-R were used to amplify a 102-bp product for *EsHSC70-3*. A constitutive expression gene (*β-actin*) was used as an internal control. Two *β-actin* primers, Qβ-actin-F and Qβ-actin-R (Table 1), were used to analyze the expression profiles of the *E. sinensis β-actin*. Negative controls missing a cDNA template were included, and the RT-qPCR was conducted using a SYBR® Premix Ex Taq™ II (TaKaRa) with a Rotor-Gene® Q (Qiagen) real-time PCR instrument.

Table 1. Primers used for gene cloning, semi-quantitative RT-PCR and real-time quantitative PCR quantification.

Application	Primer	Primer sequence (5'→3')	Amplicon length (bp)	
5'-RACE	5'-RACE Abridged Anchor Primer	5'-GGCCACGGGTCCGACTAGTACGGGGGGGGG-3'		
	AUAP	5'-GGCCACGGGTCCGACTAGTAC-3'		
	UAP	5'-CUACUACUACUAGGCCACGGTCCGACTAGTAC-3'		
	5'-RACE Anchor Primer	5'-CUACUACUACUAGGCCACGGTCCGACTAGTACGGGGGGGGG-3'		
	HSC705-GSP51	5'-GTGAATGATGTCTCTCGCCCTG-3'	1905	
	HSC705-GSP52	5'-TCTCCATCTTGCTCTCTGTG-3'	1928	
	HSC705-GSP53	5'-CCCTGTAGCCAAGAG-3'	2011	
	HSC703-GSP1	5'-CCTTGTCTTCACCTG-3'	1884	
	HSC703-GSP2	5'-TTCAGACTGTAGGCATAGGACT-3'	1864	
	HSC703-GSP3	5'-TTCACCCTTCTTCAGCTC-3'	1826	
	3'-RACE	3'-RACE 10X Universal Primer A Mix (UPM)	5'-CTAATACGACTCACTATAGGGCAAGCAGTGGTATCAACGCAGAGT-3'	
		HSP705-GSP31	5'-GAGGAGAGAGCATCTACGACACAGAG-3'	677
		HSP705-GSP32	5'-GGAACCTTGGCTAAGAGGACTCGGCA-3'	572
HSC703-31		5'-GGACCTGAGGCTTTTGTGTGATGAGGAT-3'	545	
HSC703-32		5'-GCTGGAGGACAACCTGATTCGATGCC-3'	362	
HSC705-QCF		5'-CATGATGTCCAGAGCGGGGT-3'	2041	
HSC705-QCR		5'-ATCCTCTACTGTGGCTATCC-3'		
HSC703-QCF		5'-CAATGAGGTGTGGGTAGCC-3'	1972	
HSC703-QCR		5'-CAAAATTACAACCTCGTCCATC-3'	301	
HSC705-F*		5'-ACAAGACGGAGGACAAAGTCAI-3'	321	
HSC705-R		5'-GTGAGGTAAGGGAGTTGATG-3'	65	
HSC703-F		5'-GAGGACAACCTGATTCGATG-3'	106	
HSC703-R		5'-ACAGTCTCCGTTCCACACTTG-3'	102	
ORF full-length confirmation SqRT-PCR Real-time qPCR	β-actin-F	5'-CCGTGACCTCACAGACTACT-3'		
	β-actin-R	5'-CGGTGGTCTGAAAGGTGTAG-3'		
	qHSC705-F	5'-GCATCATCCAGCACACAGAGAG-3'		
	qHSC705-R	5'-AAGAGTCTTCACCTGTTC-3'		
	qHSC703-F	5'-ACCCACGAAGGAGTGTAT-3'		
	qHSC703-R	5'-TTTGATTTCCAGATGACTGTTG-3'		
	Qβ-actin-F	5'-CTCCTGCTGTGATCCACATC-3'		
	Qβ-actin-R	5'-GCATCCACGAGACACTTACA-3'		

F: forward primer; R: reverse primer.

The RT-qPCR amplifications were conducted in triplicate on a 96-well plate and in a 20- μ L reaction volume per well, which consisted of 10 μ L 2X SYBR[®] Premix Ex Taq[™] II (TaKaRa), 0.8 μ L 10 μ M PCR forward primer, 0.8 μ L 10 μ M PCR reverse primer, 2.0 μ L cDNA template, and 6.4 μ L sterile deionized water. The thermal profile for SYBR[®] Green RT-qPCR consisted of an initial step at 95°C for 30 s, followed by 40 cycles at 95°C for 5 s and 51°C (51°C for *EsHSC70-5* and 55°C for *EsHSC70-3*) for 30 s. SqRT-PCR primers (Table 1) were selected to produce a 301-bp amplicon for *EsHSC70-5* and a 321-bp amplicon for *EsHSC70-3*. SqRT-PCR was performed in a final volume of 30 μ L that consisted of 15 μ L 2X Taq PCR Master Mix (Lifefeng, China), 0.7 μ L 20 mM primer, 12.2 μ L sterile deionized water, and 1.4 μ L first-strand cDNA as a template. The PCR conditions were as follows: 25 cycles at 95°C for 30 s, 53°C for 30 s, and 72°C for 50 s. Internal control PCRs for *β -actin* were performed in a separate tube as described above, with the exception of an alternative gene-specific primer pair (β -actin-R and β -actin-F; Table 1), which was designed based upon a cloned *E. sinensis* *β -actin* cDNA fragment (GenBank accession No. AY910691) to produce a 65-bp amplicon. All of the SqRT-PCRs were completed in triplicate using independently extracted RNA. SqRT-PCR products were size-separated on an ethidium bromide-stained 1.5% agarose gel, visualized under ultraviolet light, and images were captured with a UVP DS7500 Gel imaging system (Upland, CA, USA).

The RT-qPCR data from the three replicated experiments, which were run to ensure the accuracy and validity of the experimental results, were then analyzed with the Rotor-Gene[®] Q Series software v.1.7.94 (Qiagen). All of the analyses were based on the C_t values of the qPCR products. To maintain consistency, the baseline was set automatically by the software. The expression levels of *EsHSC70-5* and *EsHSC70-3* were calculated by the $2^{-\Delta\Delta C_t}$ comparative method, and the data were assessed for statistical significance using SPSS v.16.0 software. The data were analyzed using a one-way analysis of variance followed by the Tukey and the *post hoc* Duncan multiple range tests, and are reported as means \pm SEMs for N = 5 crabs per group. $P \leq 0.05$ was considered statistically significant. All values with n-fold differential expression were plotted on a graph.

***EsHSC70-5* and *EsHSC70-3* sequence analysis**

The full-length cDNA sequences were subjected to a homology analysis using the National Center for Biotechnology Information (NCBI) Basic Local Alignment Search Tool (BLAST) database. The resulting sequences were verified and subjected to cluster analysis. The *EsHSC70-5* and *EsHSC70-3* amino acid sequences, plus other HSC70 and HSP70 amino acid sequences retrieved from the NCBI protein database ([Table S2](#)), were subjected to ClustalW2 for multiple sequence alignment. Multiple sequence alignment was performed with the ClustalW2 Multiple Alignment program on the EMBL-EBI website. The ORFs of the *EsHSC70-5* and *EsHSC70-3* cDNAs were determined using ORF Finder. The molecular mass and theoretical isoelectric point were predicted using the Compute pI/Mw tool. A motif scan was performed in motif databases and by the Simple Modular Architecture Research Tool (SMART). The putative signal peptide was predicted using the SignalP 4.1 Server, and the potential protein subcellular localization was predicted by PSORT II. The three-dimensional domain structures of *EsHSC70-5* and *EsHSC70-3* were predicted by SWISS-MODEL. Additional assessments of domain structures were performed using ProSA-web and Verify_3D. Transmembrane topology prediction was performed using the TMHMM Server v. 2.0 and the DAS-TMfilter server. All of the analytical procedure URLs are available in [Table S3](#).

RESULTS

Identification and characterization of full-length cDNAs encoding *EsHSC70-5* and *EsHSC70-3*

Several fragments (1905, 1928, and 2011 bp for *EsHSC70-5*; 1884, 1864, and 1826 bp for *EsHSC70-3*) were amplified by the 5'-RACE technique from the 5' end of each cDNA, and several fragments (677 and 572 bp for *EsHSC70-5*, 545 and 362 bp for *EsHSC70-3*) were amplified by the 3'-RACE technique. The ORF full-length cDNA sequence validation produced a 2041-bp fragment for *EsHSC70-5* and a 1972-bp fragment for *EsHSC70-3*.

The sequence data indicated a 2563-bp full-length *EsHSC70-5* cDNA with a 1905-bp ORF starting at nucleotide 159 and stopping at nucleotide 2176, which encodes 634 amino acid residues with a putative molecular mass of 73.7 kDa and a calculated theoretical isoelectric point of 5.48, and a 2314-bp full-length *EsHSC70-3* cDNA with a 1965-bp ORF starting at nucleotide 145 and stopping at nucleotide 2109, which encodes 654 amino acid residues with a deduced molecular mass of 72.3 kDa and a calculated theoretical isoelectric point of 4.95. The *EsHSC70-5* cDNA included a 144-bp 5'-terminal untranslated region (UTR) and a 385-bp 3'-UTR, while the *EsHSC70-3* cDNA included a 144-bp 5'-UTR and a 205-bp 3'-UTR. In addition, stop codons (TAG in *EsHSC70-5* and TAA in *EsHSC70-3*), canonical polyadenylation signals (AATAAA located at nucleotide 2529 in *EsHSC70-5* and at nucleotide 2281 in *EsHSC70-3*), and poly-(A) tails were found in the 3' end of the *EsHSC70-5* and *EsHSC70-3* cDNAs ([Figure S1A](#) and [B](#)). TGTnACA consensus sequences (27-33 nt and 180-186 nt) and several putative transcription factor-binding sites, such as ten E-box (CANNTG) motifs, were identified in the *EsHSC70-3* cDNA [one was located in the 5'-UTR (124-129 nt), eight were located in the ORF (391-396, 529-534, 644-649, 1531-1536, 1669-1674, 1864-1869, 1947-1952, and 2054-2059 nt), and one was located in the 3'-UTR (2255-2260 nt)] (Park et al., 2001). Seven E-box (CANNTG) motifs were identified in the *EsHSC70-5* cDNA, six were located in the ORF (686-691, 977-982, 1156-1161, 1543-1548, 1556-1561, and 1939-1944 nt) and one was located in the 3'-UTR (2375-2380 nt). The deduced amino acid sequences of *EsHSC70-5* and *EsHSC70-3* revealed several canonical features of the HSC70 family. Three HSP70 protein family signature sequences, including IDLGTTNS (aa 54-61 in *EsHSC70-5*) or IDLGTTYs (aa 33-40 in *EsHSC70-3*), VYDLGGGTFDVSIL (aa 239-252 in *EsHSC70-5*) or VFDLGGGTFDVSLL (aa 221-234 in *EsHSC70-3*), and VILVGGMSRVPKVIS (aa 380-394 in *EsHSC70-5*) or IVLVGGSTRIPKIQQ (aa 358-372 in *EsHSC70-3*) (Zdobnov and Apweiler, 2001; Sonoda et al., 2006) were identified in most of the individuals sampled ([Figures S1A](#) and [B](#), [S2](#), and [S3](#)). In addition, other typical motifs were found in the *EsHSC70-5* and *EsHSC70-3* sequences ([Figure S1A](#) and [B](#)). The first was a deduced ATP-GTP binding site, GEAYLNTP (aa 175-182) (Sonoda et al., 2006) in *EsHSC70-5*, and AEAYLGKT (aa 156-163) (Sonoda et al., 2006) in *EsHSC70-3*. The second was a non-organellar consensus motif, RAKFEEL (aa 323-329) (Tungjitwitayakul et al., 2008) in *EsHSC70-3*. The C+G content of the *EsHSC70-5* and *EsHSC70-3* cDNAs was 51.66 and 48.88%, respectively. Multiple sequence alignment revealed that the deduced amino acid sequences of *EsHSC70-5* and *EsHSC70-3* exhibited more than 45 and 57% identity, respectively, to their corresponding sequences in other species ([Figure S4](#) and [Table S2](#)). The 2564 and 2315-bp nucleotide sequences represented the full-length cDNA sequences of *EsHSC70-5* and *EsHSC70-3*, respectively. The full-length *EsHSC70-5* and *EsHSC70-3* cDNA sequences were assigned the GenBank accession Nos. KC493625 and KC493626, respectively.

Structural analysis of EsHSC70-5 and EsHSC70-3

No signal sequence was identified in the EsHSC70-5 transcript, whereas a signal sequence was identified in the EsHSC70-3 transcript using SignalP ([Figures S1B](#) and [S3](#)). The results from BLASTp in NCBI indicated that both the EsHSC70-5 and EsHSC70-3 proteins have a HSP70 family domain, with multiple nucleotide binding sites, ATP-GTP binding sites, and protein interaction sites ([Figures S2](#) and [S3](#)). Protein motif-domain scanning by SMART revealed that EsHSC70-5 and EsHSC70-3 contain a HSP70 domain (from 54 to 653 amino acid residues for EsHSC70-5 and from 30 to 635 amino acid residues for EsHSC70-3). EsHSC70-5 contained three N-glycosylation sites, one amidation site, one cAMP- and cGMP-dependent protein kinase phosphorylation site, fifteen casein kinase II phosphorylation sites, one leucine zipper pattern, ten protein kinase C phosphorylation sites, and one tyrosine kinase phosphorylation site ([Figure S1A](#)). EsHSC70-3 contained fourteen casein kinase II phosphorylation sites, the endoplasmic reticulum-targeting sequence “KDEL”, eight protein kinase C phosphorylation sites, and one tyrosine kinase phosphorylation site ([Figure S1B](#)). Three-dimensional structural analysis of EsHSC70-5 revealed that it contains two clearly distinguishable domains attached to each other by a relatively flexible loop. A highly twisted, ten-stranded β -sheet was covered on one side by five α -helices in the C-terminal domain, whereas sixteen-stranded β -sheets were covered inside by fourteen α helices in the NH2-terminal domain. A similar X-ray crystal structure of bovine HSC70 has been reported (Schuermann et al., 2008). Nests, such as GLY175, GLU176, ALA177, TYR178, LEU179, ASN180, THR181, and PRO182, were located in these α -helices and loop chains, which form ATP-GTP binding sites (see [Figure S5A](#)). The overall model quality (Z-score) was -10.32, and local model quality values were generally below zero. The average 3D-1D score ranged from -0.02 to 0.71. The predicted three-dimensional structure of EsHSC70-3 possessed a common α/β fold. These 29 highly twisted, stranded β -sheets were covered inside by 14 α -helices. Some important structural motifs, including ATP-GTP binding sites (such as ALA156, GLU157, ALA158, TYR159, LEU160, GLY161, LYS162, and THR163) and non-organellar consensus motifs (such as ARG323, ALA324, LYS325, PHE326, GLU327, GLU328, and LEU329) that were located in the α -helices and loop chains were identified ([Figure S5B](#)). The Z-score for the overall model quality was -11.16, and local model quality values for all residues were generally below zero according to ProSA-Web. The 3D-1D average score obtained from Verify_3D ranged from -0.04 to 0.77. The quality evaluation results of the predicted three-dimensional structure of EsHSC70-5 and EsHSC70-3 indicated that they were accurate and valid.

A transmembrane topology prediction indicated that EsHSC70-5 and EsHSC70-3 are probably non-transmembrane proteins. The potential protein subcellular localization prediction indicated that EsHSC70-5 is probably located in the cytoplasm (39.1%), while EsHSC70-3 is probably located in the endoplasmic reticulum (44.4%). The SignalP prediction indicated that both EsHSC70-5 and EsHSC70-3 are non-secretory proteins.

Expression analysis of *EsHSC70-5* and *EsHSC70-3* mRNA during larval brachyurization

The mRNA expression levels of *EsHSC70-5* and *EsHSC70-3* in the embryo and in nine larval stages of *E. sinensis* were analyzed by SqRT-PCR and RT-qPCR. The relative expression levels of the two *EsHSC70* mRNAs at the embryo stage were used as a calibrator and set at 1.0.

The relative mRNA expression levels of *EsHSC70-5* and *EsHSC70-3* at different larval stages were indicated as n-fold differences relative to the calibrator. As determined by RT-qPCR and SqRT-PCR, the mRNA transcripts of *EsHSC70-5* and *EsHSC70-3* were frequently detected and differentially expressed at different juvenile stages of *E. sinensis* (Figure 1), and the internal control constitutive expression gene, β -actin, was consistently expressed at different juvenile stages (Figures 1-B, D). It was clear that the expression profile of *EsHSC70-5* was quite similar to that of *EsHSC70-3* at all of the developmental stages. The highest *EsHSC70-5* mRNA levels appeared at stage Z2, whereas the highest expressive *EsHSC70-3* transcript was found at stage Z1 ($P < 0.05$). The lowest level of expression for *EsHSC70-5* was detected at stage J2. The *EsHSC70-5* mRNA expression level increased at first and then decreased from stages O to Z5, and then slightly increased at stages M and J1. *EsHSC70-5* was significantly downregulated at stage J2 (~6.1-fold lower than that at stage J1, $P < 0.05$), and slightly upregulated at stage J3 (Figure 1A). Similarly, the *EsHSC70-3* mRNA expression level increased at first and then decreased from stages O to Z5, and the lowest level of expression appeared at stage Z5. *EsHSC70-3* was significantly upregulated at stage M (~6.9-fold higher than that at stage Z5, $P < 0.01$), slightly downregulated from stages M to J2, and finally slightly upregulated at stage J3 (~1.6-fold higher than that at stage J2, $P > 0.05$) (Figure 1C). The SqRT-PCR results confirmed those obtained by RT-qPCR (Figures 1B and D).

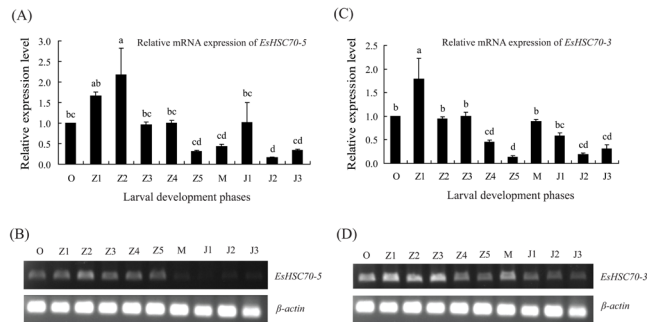


Figure 1. Relative *EsHSC70-5* and *EsHSC70-3* expression levels ($2^{-\Delta\Delta C_t}$) in *Eriocheir sinensis* larvae at different developmental stages. **A.** **B.** *EsHSC70-5* (A) and *EsHSC70-3* (B) mRNA expression levels were detected by RT-qPCR. Bars represent means \pm SE (N = 3). Statistical significance is indicated with lowercase letters (Tukey's *post hoc* test, $\alpha = 0.05$). **C.** **D.** *EsHSC70-5* (C) and *EsHSC70-3* (D) mRNA expression profiles were detected by SqRT-PCR. O (embryo stage), Z1 (the first zoeal stage), Z2 (the second zoeal stage), Z3 (the third zoeal stage), Z4 (the fourth zoeal stage), Z5 (the fifth zoeal stage), M (megalopa stage), J1 (the first juvenile crab stage), J2 (the second juvenile crab stage), and J3 (the third juvenile crab stage). β -actin gene is used as an internal control.

EsHSC70-5 and *EsHSC70-3* expression profiles after *V. parahaemolyticus* challenge

The expression patterns of *EsHSC70-5* and *EsHSC70-3* mRNA were examined at 6, 12, 24, 36, and 48 h after an immune challenge (Figures 2 and 3) in different tissues (Figures 4 and 5), and in controls that were not immune challenged. Following the RT-qPCR, the dissociation curves of *EsHSC70-5*, *EsHSC70-3*, and β -actin (internal control) exhibited a single, sharp peak, which confirmed that the amplifications were specific. The expression levels of *EsHSC70-5* and *EsHSC70-3* mRNA in the blank controls were used as a calibrator and set at 1.0. As determined by RT-qPCR, *EsHSC70-5* and *EsHSC70-3* were widely expressed in all of the sampled tissues of healthy and immune-challenged crabs, but their levels differed between the

bacterially infected tissues (Figures 2-5). The expression levels of *EsHSC70-5* and *EsHSC70-3* mRNA in all of the tissues were significantly induced by *V. parahaemolyticus* at 6 to 48 h post-injection compared to the controls (Figures 2 and 3). *EsHSC70-5* and *EsHSC70-3* expression fluctuated at all of the time points in all of the tissues, but was maintained at a relatively high level in the hepatopancreas. *EsHSC70-5* in the heart was significantly upregulated at 12 h (~2.3-fold higher than that in the controls, $P < 0.01$), significantly downregulated at 24 and 48 h compared to the controls, and stabilized to near-normal levels at 6 and 36 h post-challenge (Figure 2A). In the hepatopancreas, *EsHSC70-5* was significantly downregulated after 6 h compared to the control ($P < 0.05$) and significantly upregulated after 12 h (~2.5-fold higher than that in the controls, $P < 0.01$). *EsHSC70-5* was then significantly downregulated at 24 h ($P < 0.05$) and reached its lowest level at 36 h post-injection compared to the controls, before being significantly upregulated at 48 h (~1.2-fold higher than that in the controls, $P < 0.05$) (Figure 2B). *EsHSC70-5* expression was significantly downregulated in the intestine and gills at nearly all of the time points compared to the controls. *EsHSC70-5* mRNA levels in the intestine slightly decreased at 6 and 24 h to 74.31 and 67.89%, respectively, of the control level. At 12, 36, and 48 h, the mRNA expression levels of *EsHSC70-5* significantly decreased to 38.99, 51.45, and 64.31%, respectively, of the control level (Figure 2C). In contrast, *EsHSC70-5* mRNA levels in the gills significantly decreased at 6 to 48 h to 5.43, 3.84, 16.04, 24.89, and 16.49%, respectively, of the control level (Figure 2D).

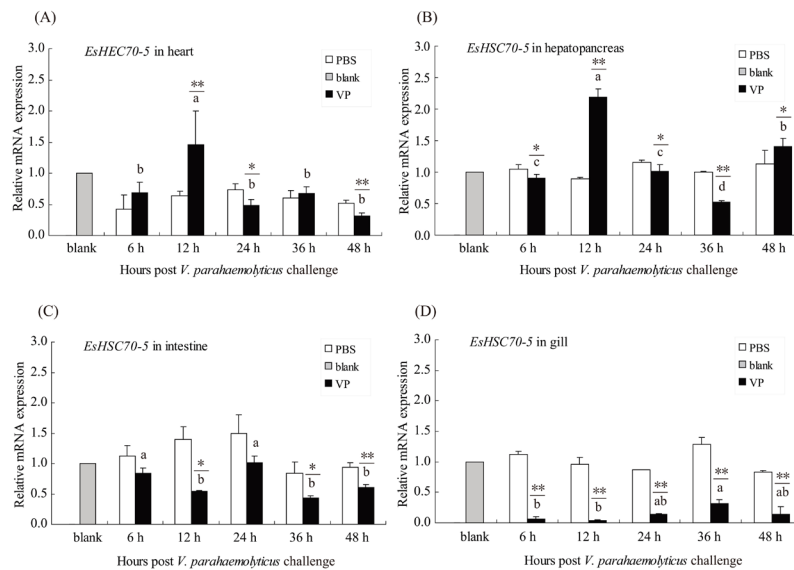


Figure 2. *EsHSC70-5* mRNA expression in heart (A), hepatopancreas (B), intestine (C), and gill (D) tissues of *Eriocheir sinensis* in response to *Vibrio parahaemolyticus* challenge (black bars). Tissues collected from crabs injected with *V. parahaemolyticus* (black bars) or PBS (white bars) and healthy crabs (gray bars) were compared with respect to *EsHSC70-5* mRNA expression (relative to β -actin) using the Tukey *post hoc* test. Bars represent mean \pm SE of three independent investigations. Statistical significance is indicated with an asterisk between tissues injection with VP and PBS. * $P < 0.05$ and ** $P < 0.01$. Different lowercase letters indicating statistical significantly among different time points post-injection with VP (Tukey's *post hoc* test, $\alpha = 0.05$). h = hours post-challenge. Blank control group (healthy crabs) was taken as the calibrator.

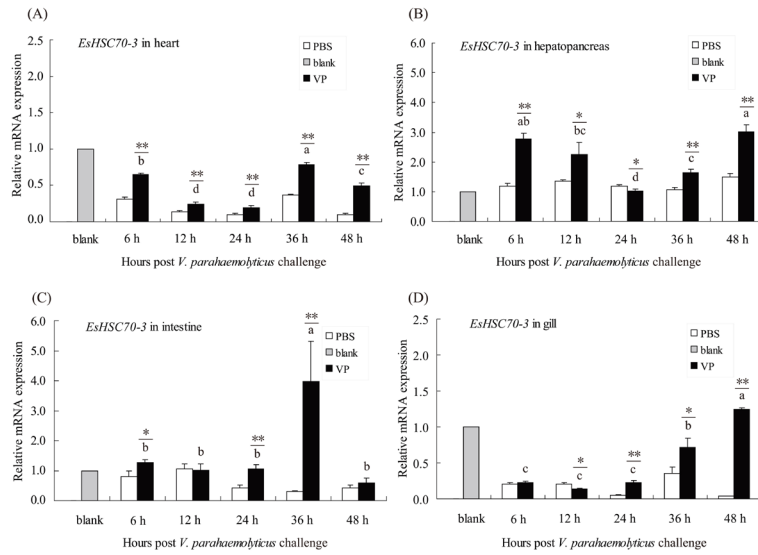


Figure 3. *EsHSC70-3* mRNA expression in heart (A), hepatopancreas (B), intestine (C), and gill (D) tissues of *Eriocheir sinensis* in response to *Vibrio parahaemolyticus* challenge (black bars) at 6 h, 12 h, 24 h, 36 h and 48 h. Tissues collected from crabs injected with *V. parahaemolyticus* (black bars) or PBS (white bars) and healthy crabs (gray bars) were compared with respect to *EsHSC70-3* mRNA expression (relative to β -actin) using Tukey's *post hoc* test. Error bars represent mean \pm SE of three independent investigations. Statistical significance is indicated with an asterisk between tissues injection with VP and PBS. * $P < 0.05$ and ** $P < 0.01$. Different lowercase letters indicating statistical significantly among different time points post-injection with VP (Tukey's *post hoc* test, $\alpha = 0.05$). h = hours post-challenge. Blank control group (healthy crabs) was taken as the calibrator.

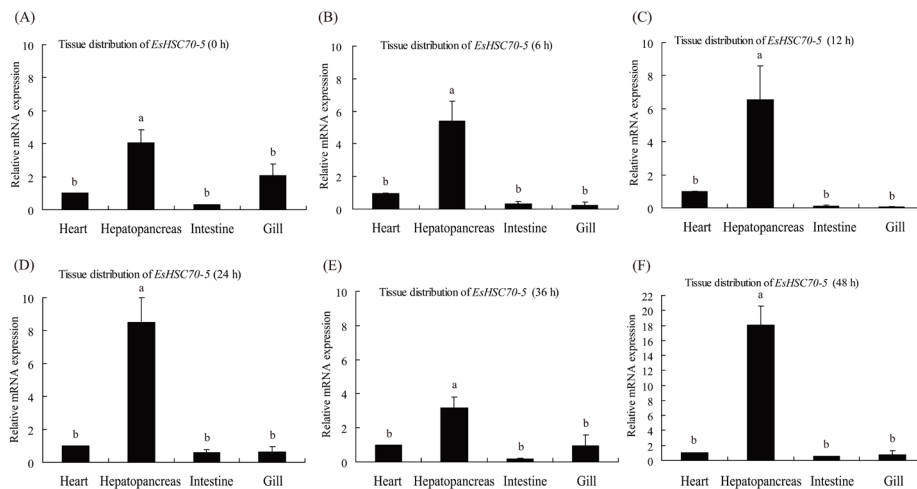


Figure 4. Tissue distribution of *EsHSC70-5* mRNA in heart, hepatopancreas, intestine, and gill tissues of *Eriocheir sinensis* at different time periods after *Vibrio parahaemolyticus* infection. Fold expression relative to β -actin was calculated as $2^{-\Delta\Delta Ct}$. h = hours post-challenge. Statistical significance is indicated with lowercase letters (Tukey's *post hoc* test, $\alpha = 0.05$).

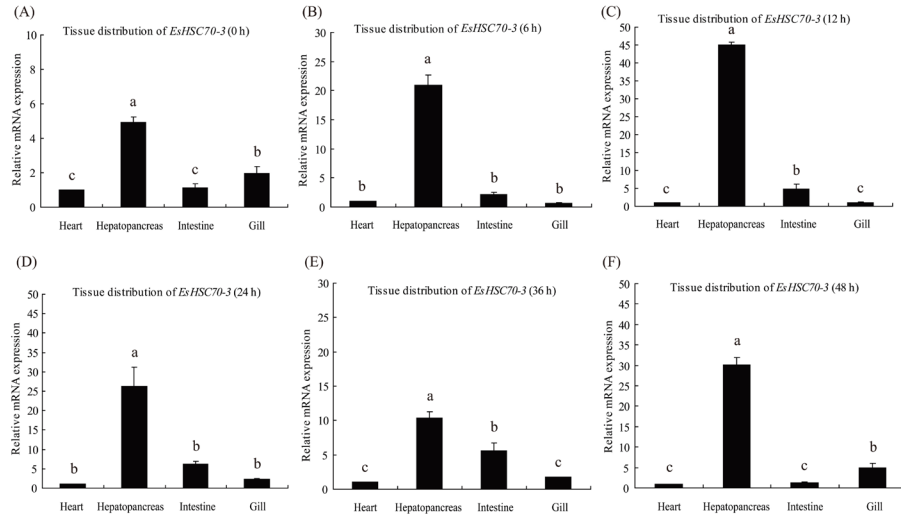


Figure 5. Tissue distribution of *EsHSC70-3* mRNA in heart, hepatopancreas, intestine, and gill tissues of *Eriocheir sinensis* at different time periods after *Vibrio parahaemolyticus* infection. Fold expression relative to β -actin was calculated as $2^{-\Delta\Delta Ct}$. h = hours post-challenge. Statistical significance is indicated with lowercase letters (Tukey's *post hoc* test, $\alpha = 0.05$).

Unlike *EsHSC70-5*, the expression level of *EsHSC70-3* was upregulated in all of the tissues at nearly all of the time points compared to the controls, except for 24 h post-challenge in the hepatopancreas and 12 h post-challenge in the intestine and gills. *EsHSC70-3* in the heart exhibited an expression pattern similar to that in the intestine, and *EsHSC70-3* in the hepatopancreas exhibited an expression pattern similar to that in the gills. In the heart and intestinal tissues, *EsHSC70-3* mRNA levels decreased at first and then significantly increased and reached a peak at 36 h, before significantly decreasing at 48 h (Figures 3A and 3C). In the hepatopancreas and gill tissues, *EsHSC70-3* mRNA expression levels decreased at first and then significantly increased, and reached their highest level at 48 h post-injection (Figures 3B and 3D). *EsHSC70-3* expression in the heart increased to 2.1-, 1.8-, 1.9, 2.1-, and 4.9-times above the control at 6, 12, 24, 36, and 48 h post-challenge, respectively (Figure 3A). *EsHSC70-3* mRNA levels in the hepatopancreas significantly decreased at 24 h to 86.56% of the control level, and it significantly increased to 2.3-, 1.7-, 1.6-, and 2.0-times above the control at 6, 12, 36, and 48 h post-challenge, respectively (Figure 3B). *EsHSC70-3* expression was almost at normal levels at 12 h, but increased to 1.6-, 2.5-, 12.9-, and 1.4-times above the control at 6, 24, 36, and 48 h post-challenge, respectively (Figure 3C). *EsHSC70-3* mRNA levels in the gills significantly decreased at 12 h to 66.46% of the control level, and increased to 1.1-, 4.7-, 2.0-, and 34.8-times above the control at 6, 24, 36, and 48 h post-challenge, respectively (Figure 3D). Significant differences ($P < 0.05$) were detected at all time points between the control and challenged groups, except at 6 and 36 h post-challenge in the heart and 6 and 24 h post-challenge in the intestine for *EsHSC70-5*, and at 12 and 48 h post-challenge in the intestine and 6 h post-challenge in the gills for *EsHSC70-3*. Although *EsHSC70-5* and *EsHSC70-3* expression levels in the control group fluctuated slightly between the different time points, few significant differences were found between them (white and gray bars in Figures 2-3). The β -actin expression level was also not affected by the challenge (data not shown).

Tissue distribution of *EsHSC70-5* and *EsHSC70-3* after *V. parahaemolyticus* challenge

The mRNA transcripts of *EsHSC70-5* and *EsHSC70-3* were detected in all of the examined tissues with different expression levels under immune challenge. The *EsHSC70-5* transcript was most abundant in the hepatopancreas, with a moderate expression level in the heart, and a low expression level in the intestine and gills (Figures 2 and 4). *EsHSC70-3* was mainly expressed in the hepatopancreas, but was also detected in the heart, intestine, and gills (Figures 3 and 5). The statistical analyses revealed that significant differences existed in the *EsHSC70-5* and *EsHSC70-3* expression levels between the tissues. *EsHSC70-5* expression levels in the hepatopancreas were significantly higher ($P < 0.01$) than those in the intestine, heart, and gills at 0 h. The lowest *EsHSC70-5* expression level was found in the intestine at 0 h (~0.07-fold lower than that in the hepatopancreas, $P < 0.01$) (Figure 4-A). *EsHSC70-5* mRNA expression in the gills was downregulated 6 h post-challenge, and reached its lowest level (~0.01-fold lower than that in the hepatopancreas, $P < 0.01$) at 12 h post-challenge (Figures 4B and C). The expression level of *EsHSC70-5* had increased in the intestine at 24 h (~1.9-fold higher than that at 12 h, $P < 0.01$) and in the gill at 24 h (~3.8-fold higher than that at 12 h) post-challenge (Figure 4D). At 36 h, the highest mRNA expression level of *EsHSC70-5* was in the hepatopancreas, while the lowest was in the intestine (Figure 4E). *EsHSC70-5* mRNA levels in the hepatopancreas and intestine increased by 2.7- and 1.4-fold, respectively, at 48 h compared to those at 36 h post-challenge. The *EsHSC70-5* mRNA level in the gills significantly decreased at 48 h to 43.12% of the level at 36 h (Figure 4F). *EsHSC70-3* expression levels in the hepatopancreas were significantly higher than those in the intestine, heart, and gills under no challenge stress ($P < 0.01$), as was the case with *EsHSC70-5*. The lowest *EsHSC70-3* expression level was found in the heart at 0 h (~0.2-fold lower than that in the hepatopancreas, $P < 0.01$). *EsHSC70-3* expression levels in the gills were significantly higher ($P < 0.05$) than those in the intestine (~0.6-fold higher) and heart (~0.5-fold higher) at 0 h (Figure 5A). After the challenge, *EsHSC70-3* mRNA expression in the gills was downregulated between 0 and 12 h, upregulated between 24 and 48 h, and reached its highest level at 48 h. At 6 h post-challenge, the highest *EsHSC70-3* mRNA expression level (~31.1-fold higher than that in the gill) was in the hepatopancreas, while the lowest was in the gills (Figure 5B). At 12 to 48 h post-challenge, the lowest *EsHSC70-3* mRNA expression levels were all in the heart. *EsHSC70-3* mRNA expression levels in the hepatopancreas were about 44.9-, 26.3-, 10.3-, and 30.1-fold higher than those in the gills at 6, 24, 36, and 48 h post-challenge, respectively (Figures 5C to 5F). In addition, *EsHSC70-3* mRNA expression levels in the intestine were significantly higher ($P < 0.01$) than those in the heart and gills at 24 and 36 h post-challenge (Figures 5C and 5E), whereas those in the gills were significantly higher ($P < 0.05$) than those in the heart and intestine at 48 h post-challenge (Figure 5-F).

DISCUSSION

HSP90, HSP70, and HSC70 are molecular chaperones that regulate protein degradation in crustaceans (Spees et al., 2003). HSC70s play essential roles in protein metabolism (Park et al., 2001), and they function as molecular chaperones or housekeeping proteins in many cellular physiological processes (Guerrero et al., 2002; Yan et al., 2010; Iwanaga et al., 2014). The identification and characterization of *HSC70s* may provide valuable information for farming freshwater crabs. In the present study, two different *HSC70s*, *EsHSC70-5* and

EsHSC70-3, were identified in *E. sinensis*. Although *HSC70* and *HSP70* have been previously identified in many species, this is the first report of HSC70 cDNAs from brachyuran decapod crustaceans. The putative protein sequences of the cloned full-length *EsHSC70-5* and *EsHSC70-3* cDNAs shared more than 45 and 57% identity, respectively, with HSC70s/HSP70s of other known arthropods (Table S2 and Figures S2 and S3). As shown in Table S2, the *EsHSC70s* exhibited a lower identity (45 to 77%) with related HSC70s/HSP70s in crustaceans than those in insect HSC70s. We have failed to find a reasonable explanation for these puzzling results. The consensus sequences TGTCACA (27-33 nt) and TGTGGCA (180-186 nt) were identified in *EsHSC70-3*. The central TGTnACA sequence is essential for muscle-specific factor recognition; although sequences flanking the central TGTnACA may also participate in binding activity within *HSC71* in *Rivulus marmoratus*, and TGTCACA has greater binding affinity than TGTGGCA (Park et al., 2001). Amino acid sequence analysis demonstrated that both of the isolated cDNAs conserved the typical structural features of eukaryotic cytoplasmic HSP70 family members (Figure S1). In addition, the *EsHSC70-5* and *EsHSC70-3* sequences included two additional specific motifs that were indicative of HSP70 cytosolic localization: a non-organellar stress protein consensus motif, RAKFEEL (aa 323-329) (Tungjitwitayakul et al., 2008), in *EsHSC70-3* and a deduced ATP-GTP binding site, GEAYLNTP (aa 175-182) (Sonoda et al., 2006) in *EsHSC70-5*, and AEAYLGKT (aa 156-163) (Sonoda et al., 2006) in *EsHSC70-3*. However, the endoplasmic reticulum-targeting sequence “KDEL” (aa 651-654) in *EsHSC70-3* indicated that it is probably located in the endoplasmic reticulum. The conserved characteristics shared with known HSC70s/HSP70s suggest that *EsHSC70-5* and *EsHSC70-3* belong to the HSP70 family, and their molecular characteristics suggest that they play important roles in binding interactional proteins and responding to stimulation, as reported in other organisms.

The results of previous studies indicate that the cognate HSC70s are present under most conditions, and may or may not be influenced by stress (Daugaard et al., 2007; Zhang and Denlinger, 2010). HSC70s play essential roles in protein metabolism, are constitutively expressed under normal conditions, and change relatively little on exposure to stressors (Park et al., 2001; Kregel, 2002). Basal *HSP70* and *HSC70* expression profiles vary with developmental stage. In the beet armyworm (*Spodoptera exigua*), *HSP70* expression is at its highest in young larvae and decreases with age (Jiang et al., 2012), whereas in the diamondback moth (*Plutella xylostella*), it is very low in fourth-instar larvae, increases in the pupae, and reaches a peak in adults (Sonoda et al., 2006). In the present study, the two *EsHSC70* mRNA transcripts appeared to be present in all of the tested larval stages, and their expression profiles were similar. *EsHSC70-5* and *EsHSC70-3* mRNA expression levels increased at first and then decreased from stages O to Z5. *EsHSC70-3* mRNA levels slightly increased at stages M and J1, were significantly upregulated at stage M compared to stage Z5, slightly downregulated from stages M to J2, and slightly upregulated at stage J3. This fluctuation in expression patterns has also been reported in other animals during development. For example, *HSC70-4* in *Drosophila melanogaster* is expressed at a high level in the embryo, larva, and adult (Perkins et al., 1990). In *Chironomus tentans*, *HSC70* expression has been observed at all developmental stages, but is slightly lower in the embryo than in the later stages (Karouna-Renier et al., 2003). Significant variations in *HSC70* expression between organs at various developmental stages of *Manduca sexta* have been reported, which suggest that *HSC70* could be involved in a negative feedback loop-regulating assembly of the ecdysone receptor complex (Rybczynski and Gilbert, 2000). The larval development of *E. sinensis* undergoing brachyurization metamorphosis (including

organizational differentiation, neuronal integration, and molting, etc.) is accomplished from the megalopa to the first juvenile crab stage (Štević, 1971). Crabs have a soft shell after molting, and are vulnerable to physiological stresses such as pathogen infections and attack by other organisms. Megalopa larvae migrate from salt to freshwater and molt into the first juvenile crabs, which is followed by several juvenile stages of metamorphosis in freshwater (Kim and Hwang, 1995). Desalination during this period would impose an osmotic stress challenge to crabs. In this study, the highest *EsHSC70* mRNA levels appeared at the embryo and early zoeal stages. The lowest *EsHSC70* mRNA levels occurred at later zoeal stages, stages J2 and J3. In *S. exigua*, basal *HSP70* expression is at its highest in young larvae and decreases with age (Jiang et al., 2012). In the present study, *EsHSC70-5* was gradually upregulated at stages M and J1, while *EsHSC70-3* was at a relatively higher level at stages Z5 and J2. In juvenile mitten crabs, *HSP70* levels under high-salinity conditions are higher than those under low-salinity conditions (Sun et al., 2012). Therefore, the high *EsHSC70* expression levels at stages M and J1 may be elicited by osmotic stress or brachyurization metamorphosis. The fact that high *EsHSC70* mRNA levels occurred at an earlier stage of larval development suggests that *EsHSC70s* may play a role in *E. sinensis* development. Previous studies have demonstrated that *HSC70* has specific developmental functions in teleosts. High muscle-specific expression of *HSC71* correlates with muscle growth and differentiation, and with adaptive responses to muscle-specific physiological stress, such as the demand for oxidative metabolism (Park et al., 2001). Liu et al. (2004) suggested that *HSC70* might play an important role in the growth and development of *M. rosenbergii*. Therefore, the stage-specific enrichment of *EsHSC70* transcripts in crabs may signify a critical role for these stress proteins during brachyurization events.

As with the *HSC70s* in *M. nipponense* after an *Aeromonas hydrophila* challenge (Xiu et al., 2014), *HSC70s* in *E. sinensis* are inducible under *V. parahaemolyticus* challenge. Previous studies have shown that *HSP70* expression levels are significantly induced by pathogen stimulation (Cui et al., 2010; Rungrasamee et al., 2010; Das et al., 2015). In this study, quantitative RT-PCR analysis revealed that the two *EsHSC70* mRNA transcripts were present in all of the tissues sampled. The differential expression profiles of *EsHSC70-5* and *EsHSC70-3* were obvious, and *EsHSC70* expression levels in different tissues varied. *EsHSC70-5* and *EsHSC70-3* expression levels fluctuated at all of the time points in all of the tissues, and were maintained at relatively high levels in the hepatopancreas.

The innate immune system is the first line of defense for invertebrates. Crustaceans can induce rapid and effective immune responses to defend themselves against most potential pathogens, and rely largely on innate immunity (Vazquez et al., 2009). The hepatopancreas, hemocytes, intestines, and gills of crustaceans are immune-associated tissues, and the hepatopancreas and hemocytes are regarded as the most important tissues involved in crustacean immunity (Jiravanichpaisal et al., 2006). In this study, we found that both *EsHSC70-5* and *EsHSC70-3* were highly expressed in the hepatopancreas, based on a tissue distribution analysis of their transcripts. The high expression profiles of *EsHSC70s* in the hepatopancreas confirm their important roles in crab innate immune responses against pathogens.

The midgut, along with the gills, represents an extremely important route of infection in crustaceans. For example, infections with *V. harveyi* are known to cause extensive pathology and tissue inflammation in the gut and hepatopancreas of shrimps (Jiravanichpaisal et al., 2010). Encapsulated pathogens are cleared from the circulation, and are often collected in the gills or hepatopancreas (Hauton, 2012). In this study, the *EsHSC70-5* mRNA transcript was significantly upregulated in the heart and hepatopancreas as early as 12 h after challenge by

V. parahaemolyticus, while the expression of *EsHSC70-5* was significantly downregulated in the intestine and gills at nearly all time points compared to the controls. However, *EsHSC70-3* expression was upregulated in all of the tissues at nearly all of the time points compared to the controls. High expression was also reported in infected crabs, clams, shrimps, and rohu, as well as during Gram-negative bacterial exposure (Cui et al., 2010; Rungrassamee et al., 2010; Das et al., 2015). *M. nipponense HSC70* transcription initially increases and then decreases after challenge by *A. hydrophila* (Xiu et al., 2014), which is similar to the pattern of *EsHSC70* transcription found in the present study. The increased initial expression may be due to the processing of bacterial antigens that were infecting the cells (Das et al., 2015). *EsHSC70-3* transcription decreased at first and then steadily increased to a peak, while that of *EsHSC70-5* fluctuated at different time points post-injection. In the heart and intestinal tissues, *EsHSC70-3* mRNA levels decreased at first and then significantly increased, and reached a peak at 36 h before significantly decreasing at 48 h post-injection. In the hepatopancreas and gill tissues, *EsHSC70-3* mRNA expression levels decreased at first and then significantly increased and reached a peak at 48 h post-injection. Similar tissue-tropic expression of *HSC70s* has been reported in turbot *Scophthalmus maximus* (Wang et al., 2013) and oriental river prawns *M. nipponense* (Xiu et al., 2014). However, in the swimming crab *Portunus trituberculatus*, *PtHSP70* expression gradually increases to a peak at 12 h in hemocytes after stimulation with *V. alginolyticus* (Cui et al., 2010), which is similar to that found with *EsHSC70-5* in the hepatopancreas in the present study, but is very different to that found with *EsHSC70-3*. The *EsHSC70-5* mRNA level was significantly downregulated in the intestine and gills at nearly all time points compared to the controls, and was expressed at a low level post-challenge. The depression of *HSP70* activity by cadmium exposure might be regulated through a cAMP-responsive regulatory pathway (Vilaboa et al., 1995), which suggests that the significant downregulation of *EsHSC70-5* in the intestine and gills may also be regulated by cAMP. The transcriptional responses of *EsHSC70-5* and *EsHSC70-3* to bacterial challenge varied in degree, but *EsHSC70-5* exhibited specific immune responses against the infectious agent, indicating that the two *HSC70* genes have distinct biological tasks and may be involved in different immune mechanisms.

In conclusion, two *HSC70* members in the Chinese mitten crab *E. sinensis*, designated as *EsHSC70-5* and *EsHSC70-3*, were identified and characterized for the first time in this study. *EsHSC70-5* and *EsHSC70-3* are ubiquitously expressed during the crab's larval stages and in adult tissues. Both *EsHSC70-5* and *EsHSC70-3* transcripts exhibited varying levels of inducibility after *V. parahaemolyticus* challenge, and different expression levels were observed during larval brachyurization metamorphosis. Based on the molecular characterization and expression results, *EsHSC70s* may be involved in anti-bacterial immune responses and contribute to brachyurization metamorphosis in crabs. The differential expression profiles of *EsHSC70-5* and *EsHSC70-3* support the hypothesis that the two *HSC70* genes have distinct biological tasks. The results presented here provide useful insights for investigating stress-related responses in *E. sinensis*. Further studies are necessary to identify additional crab *HSP70s*, and to investigate their innate immune responses to different environmental and physiological stresses.

Conflicts of interest

The authors declare no conflict of interest.

ACKNOWLEDGMENTS

The authors are grateful to Dongxi Shen (Xinghua County, Jiangsu, China) and Jin Huang (Rudong County, Jiangsu, China) for providing the Chinese mitten crab material. Reserach supported by grants from the National Natural Science Foundation of China (Grant #31000954), the Program of National Science Research of Jiangsu Higher Education Institutions of China (Grant #13KJB180008 and #15KJD180005), the Research Fund for the Doctoral Program of Higher Education of China (Grant #20103207120007), and the Priority Academic Program Development of Jiangsu Higher Education Institutions.

REFERENCES

- Altschul SF, Madden TL, Schäffer AA, Zhang J, et al. (1997). Gapped BLAST and PSI-BLAST: a new generation of protein database search programs. *Nucleic Acids Res.* 25: 3389-3402. <http://dx.doi.org/10.1093/nar/25.17.3389>
- Arnold K, Bordoli L, Kopp J and Schwede T (2006). The SWISS-MODEL workspace: a web-based environment for protein structure homology modelling. *Bioinformatics* 22: 195-201. <http://dx.doi.org/10.1093/bioinformatics/bti770>
- Bausero MA, Gastpar R, Multhoff G and Asea A (2005). Alternative mechanism by which IFN-gamma enhances tumor recognition: active release of heat shock protein 72. *J. Immunol.* 175: 2900-2912. <http://dx.doi.org/10.4049/jimmunol.175.5.2900>
- Behnke J and Hendershot LM (2014). The large Hsp70 Grp170 binds to unfolded protein substrates *in vivo* with a regulation distinct from conventional Hsp70s. *J. Biol. Chem.* 289: 2899-2907. <http://dx.doi.org/10.1074/jbc.M113.507491>
- Benkert P, Biasini M and Schwede T (2011). Toward the estimation of the absolute quality of individual protein structure models. *Bioinformatics* 27: 343-350. <http://dx.doi.org/10.1093/bioinformatics/btq662>
- Bowie JU, Lüthy R and Eisenberg D (1991). A method to identify protein sequences that fold into a known three-dimensional structure. *Science* 253: 164-170. <http://dx.doi.org/10.1126/science.1853201>
- Cserző M, Eisenhaber F, Eisenhaber B and Simon I (2002). On filtering false positive transmembrane protein predictions. *Protein Eng.* 15: 745-752. <http://dx.doi.org/10.1093/protein/15.9.745>
- Chan SF, He JG, Chu KH and Sun CB (2014). The shrimp heat shock cognate 70 functions as a negative regulator in vitellogenin gene expression. *Biol. Reprod.* 91: 14. <http://dx.doi.org/10.1095/biolreprod.113.117200>
- Cheng W, Shiu YL, Guei WC, Yeh SP, et al. (2013). High mortality of broodstock of Chinese mitten crab, *Eriocheir sinensis*, infected by *Vibrio parahaemolyticus* in a reproductive period. *J. Fish. Soc. Taiwan* 40: 1-9.
- Chichester L, Wylie AT, Craft S and Kavanagh K (2015). Muscle heat shock protein 70 predicts insulin resistance with aging. *J. Gerontol. A Biol. Sci. Med. Sci.* 70: 155-162. <http://dx.doi.org/10.1093/gerona/glu015>
- Cui Z, Liu Y, Luan W, Li Q, et al. (2010). Molecular cloning and characterization of a heat shock protein 70 gene in swimming crab (*Portunus trituberculatus*). *Fish Shellfish Immunol.* 28: 56-64. <http://dx.doi.org/10.1016/j.fsi.2009.09.018>
- Das S, Mohapatra A and Sahoo PK (2015). Expression analysis of heat shock protein genes during *Aeromonas hydrophila* infection in rohu, *Labeo rohita*, with special reference to molecular characterization of Grp78. *Cell Stress Chaperones* 20: 73-84. <http://dx.doi.org/10.1007/s12192-014-0527-2>
- Daugaard M, Rohde M and Jäättelä M (2007). The heat shock protein 70 family: Highly homologous proteins with overlapping and distinct functions. *FEBS Lett.* 581: 3702-3710. <http://dx.doi.org/10.1016/j.febslet.2007.05.039>
- Gasteiger E, Hoogland C, Gattiker A, Duvaud S, et al. (2005). Protein identification and analysis tools on the ExPASy Server. In: Walker JM (ed): *The Proteomics Protocols Handbook*. Humana Press, New Jersey 571-607.
- Guerrero CA, Bouyssouade D, Zárata S, Isa P, et al. (2002). Heat shock cognate protein 70 is involved in rotavirus cell entry. *J. Virol.* 76: 4096-4102. <http://dx.doi.org/10.1128/JVI.76.8.4096-4102.2002>
- Hauton C (2012). The scope of the crustacean immune system for disease control. *J. Invertebr. Pathol.* 110: 251-260. <http://dx.doi.org/10.1016/j.jip.2012.03.005>
- Iwanaga M, Shibano Y, Ohsawa T, Fujita T, et al. (2014). Involvement of HSC70-4 and other inducible HSPs in *Bombyx mori* nucleopolyhedrovirus infection. *Virus Res.* 179: 113-118. <http://dx.doi.org/10.1016/j.virusres.2013.10.028>
- Jiang X, Zhai H, Wang L, Luo L, et al. (2012). Cloning of the heat shock protein 90 and 70 genes from the beet armyworm, *Spodoptera exigua*, and expression characteristics in relation to thermal stress and development. *Cell Stress Chaperones* 17: 67-80. <http://dx.doi.org/10.1007/s12192-011-0286-2>
- Jiravanichpaisal P, Lee BL and Söderhäll K (2006). Cell-mediated immunity in arthropods: hematopoiesis, coagulation, melanization and opsonization. *Immunobiology* 211: 213-236. <http://dx.doi.org/10.1016/j.imbio.2005.10.015>

- Jiravanichpaisal P, Söderhäll K and Söderhäll I (2010). Inflammation in arthropods. *Curr. Pharm. Des.* 16: 4166-4174. <http://dx.doi.org/10.2174/138161210794519165>
- Karouna-Renier NK, Yang WJ and Rao KR (2003). Cloning and characterization of a 70 kDa heat shock cognate gene (HSC70) from two species of *Chironomus*. *Insect Mol. Biol.* 12: 19-26. <http://dx.doi.org/10.1046/j.1365-2583.2003.00383.x>
- Kim CH and Hwang SG (1995). The complete larval development of the mitten crab *Eriocheir sinensis* H. Milne Edwards, 1853 (Decapoda, Brachyura, Grapsidae) reared in the laboratory and a key to the known zoeae of the Varuninae. *Crustaceana* 68: 793-812. <http://dx.doi.org/10.1163/156854095X02023>
- Kregel KC (2002). Heat shock proteins: modifying factors in physiological stress responses and acquired thermotolerance. *J. Appl. Physiol.* 92: 2177-2186. <http://dx.doi.org/10.1152/japplphysiol.01267.2001>
- Letunic I, Doerks T and Bork P (2012). SMART 7: recent updates to the protein domain annotation resource. *Nucleic Acids Res.* 40: D302-D305. <http://dx.doi.org/10.1093/nar/gkr931>
- Liu J, Yang WJ, Zhu XJ, Karouna-Renier NK, et al. (2004). Molecular cloning and expression of two *HSP70* genes in the prawn, *Macrobrachium rosenbergii*. *Cell Stress Chaperones* 9: 313-323. <http://dx.doi.org/10.1379/CSC-40R.1>
- Lüthy R, Bowie JU and Eisenberg D (1992). Assessment of protein models with three-dimensional profiles. *Nature* 356: 83-85. <http://dx.doi.org/10.1038/356083a0>
- Nielsen H and Krogh A (1998). Prediction of signal peptides and signal anchors by a hidden Markov model. *Proc. Int. Conf. Intell. Syst. Mol. Biol.* 6: 122-130.
- Park JH, Lee JJ, Yoon S, Lee JS, et al. (2001). Genomic cloning of the Hsc71 gene in the hermaphroditic teleost *Rivulus marmoratus* and analysis of its expression in skeletal muscle: identification of a novel muscle-preferred regulatory element. *Nucleic Acids Res.* 29: 3041-3050. <http://dx.doi.org/10.1093/nar/29.14.3041>
- Perkins LA, Doctor JS, Zhang K, Stinson L, et al. (1990). Molecular and developmental characterization of the heat shock cognate 4 gene of *Drosophila melanogaster*. *Mol. Cell. Biol.* 10: 3232-3238. <http://dx.doi.org/10.1128/MCB.10.6.3232>
- Petersen TN, Brunak S, von Heijne G and Nielsen H (2011). SignalP 4.0: discriminating signal peptides from transmembrane regions. *Nat. Methods* 8: 785-786. <http://dx.doi.org/10.1038/nmeth.1701>
- Runggrasamee W, Leelatanawit R, Jiravanichpaisal P, Klinbunga S, et al. (2010). Expression and distribution of three heat shock protein genes under heat shock stress and under exposure to *Vibrio harveyi* in *Penaeus monodon*. *Dev. Comp. Immunol.* 34: 1082-1089. <http://dx.doi.org/10.1016/j.dci.2010.05.012>
- Rybczynski R and Gilbert LI (2000). cDNA cloning and expression of a hormone-regulated heat shock protein (hsc 70) from the prothoracic gland of *Manduca sexta*. *Insect Biochem. Mol. Biol.* 30: 579-589. [http://dx.doi.org/10.1016/S0965-1748\(00\)00031-X](http://dx.doi.org/10.1016/S0965-1748(00)00031-X)
- Sigrist CJ, Cerutti L, de Castro E, Langendijk-Genevaux PS, et al. (2010). PROSITE, a protein domain database for functional characterization and annotation. *Nucleic Acids Res.* 38: D161-D166. <http://dx.doi.org/10.1093/nar/gkp885>
- Sippl MJ (1993). Recognition of errors in three-dimensional structures of proteins. *Proteins* 17: 355-362. <http://dx.doi.org/10.1002/prot.340170404>
- Schuermann JP, Jiang J, Cuellar J, Llorca O, et al. (2008). Structure of the Hsp110:Hsc70 nucleotide exchange machine. *Mol. Cell* 31: 232-243. <http://dx.doi.org/10.1016/j.molcel.2008.05.006>
- Sonoda S, Ashfaq M and Tsumuki H (2006). Cloning and nucleotide sequencing of three heat shock protein genes (*hsp90*, *hsc70*, and *hsp19.5*) from the diamondback moth, *Plutella xylostella* (L.) and their expression in relation to developmental stage and temperature. *Arch. Insect Biochem. Physiol.* 62: 80-90. <http://dx.doi.org/10.1002/arch.20124>
- Spees JL, Chang SA, Mykles DL, Snyder MJ, et al. (2003). Molt cycle-dependent molecular chaperone and polyubiquitin gene expression in lobster. *Cell Stress Chaperones* 8: 258-264. [http://dx.doi.org/10.1379/1466-1268\(2003\)008<0258:MCMCAP>2.0.CO;2](http://dx.doi.org/10.1379/1466-1268(2003)008<0258:MCMCAP>2.0.CO;2)
- Štević Z (1971). The main features of brachyuran evolution. *Syst. Zool.* 20: 331-340. <http://dx.doi.org/10.2307/2412345>
- Sun M, Jiang K, Zhang F, Zhang D, et al. (2012). Effects of various salinities on Na^{+} - K^{+} -ATPase, *Hsp70* and *Hsp90* expression profiles in juvenile mitten crabs, *Eriocheir sinensis*. *Genet. Mol. Res.* 11: 978-986. <http://dx.doi.org/10.4238/2012.April.19.3>
- Tirolì-Cepeda AO, Lima TB, Balbuena TS, Gozzo FC, et al. (2014). Structural and functional characterization of the chaperone Hsp70 from sugarcane. Insights into conformational changes during cycling from cross-linking/mass spectrometry assays. *J. Proteomics* 104: 48-56. <http://dx.doi.org/10.1016/j.jprot.2014.02.004>
- Tungjitwitayakul J, Tatum N, Singtripop T and Sakurai S (2008). Characteristic expression of three heat shock-responsive genes during larval diapause in the bamboo borer *Omphisa fuscidentalis*. *Zoolog. Sci.* 25: 321-333. <http://dx.doi.org/10.2108/zsj.25.321>
- Vazquez L, Alpuche J, Maldonado G, Agundis C, et al. (2009). Review: Immunity mechanisms in crustaceans. *Innate Immun.* 15: 179-188. <http://dx.doi.org/10.1177/1753425909102876>

- Vilaboa NE, Calle C, Pérez C, de Blas E, et al. (1995). cAMP increasing agents prevent the stimulation of heat-shock protein 70 (HSP70) gene expression by cadmium chloride in human myeloid cell lines. *J. Cell Sci.* 108: 2877-2883.
- Wan XH, Pei HS, Shen HS, Jin Y, et al. (2000). Isolation and diagnosis of the pathogenic vibrio in the system of cultivating river crab larva in the south of Jiangsu province. *J. Aquaculture* 1: 19-21.
- Wang TT, Wang N, Liao XL, Meng L, et al. (2013). Cloning, molecular characterization and expression analysis of heat shock cognate 70 (*Hsc70*) cDNA from turbot (*Scophthalmus maximus*). *Fish Physiol. Biochem.* 39: 1377-1386. <http://dx.doi.org/10.1007/s10695-013-9792-8>
- Wiederstein M and Sippl MJ (2007). ProSA-web: interactive web service for the recognition of errors in three-dimensional structures of proteins. *Nucleic Acids Res.* 35: W407-10. <http://dx.doi.org/10.1093/nar/gkm290>
- Xiu Y, Feng J, Lu W, Liu D, et al. (2014). Identification of a novel cognate cytosolic Hsp70 gene (MnHsc70-2) from oriental river prawn *Macrobrachium nipponense* and comparison of its expressions with the first cognate Hsc70 (MnHsc70-1) under different stresses. *Cell Stress Chaperones* 19: 949-961. <http://dx.doi.org/10.1007/s12192-014-0519-2>
- Xu HS, Shu MA, Zhan XA and Wang SX (2002). Identification of *Vibrio parahaemolyticus* isolated from cultured *Eriocheir sinensis* and pathogenicity of its extracellular products. *J. Fisheries China* 26: 357-362.
- Yan F, Xia D, Hu J, Yuan H, et al. (2010). Heat shock cognate protein 70 gene is required for prevention of apoptosis induced by WSSV infection. *Arch. Virol.* 155: 1077-1083. <http://dx.doi.org/10.1007/s00705-010-0686-0>
- Zdobnov EM and Apweiler R (2001). InterProScan--an integration platform for the signature-recognition methods in InterPro. *Bioinformatics* 17: 847-848. <http://dx.doi.org/10.1093/bioinformatics/17.9.847>
- Zhang Q and Denlinger DL (2010). Molecular characterization of heat shock protein 90, 70 and 70 cognate cDNAs and their expression patterns during thermal stress and pupal diapause in the corn earworm. *J. Insect Physiol.* 56: 138-150. <http://dx.doi.org/10.1016/j.jinsphys.2009.09.013>

Supplementary material

Figure S1. Structures of full-length cDNA sequences and deduced amino acid sequences of (A) EsHSC70-5, (B) EsHSC70-3 in *Eriocheir sinensis*. The putative polyadenylation signals (AATAAA) are marked in green and bold. The stop codons are indicated by asterisk (*). Sequences of the primers used for obtaining open reading frame fragments (HSC705-QCF and HSC705-QCR for EsHSC70-5, HSC703-QCF and HSC703-QCR for EsHSC70-3) and RACE products (HSC705-GSP51/HSC705-GSP52/HSC705-GSP53 and HSC705-GSP31/HSC705-GSP32 for EsHSP70-5, HSC703-GSP1/HSC703-GSP2/HSC703-GSP3 and HSC703-31/HSC703-32 for EsHSC70-3) are underlined and arrowed from the 5'- to 3'-end. Three HSP70 family signatures sequences in EsHSC70-5 and EsHSC70-3 are boxed, respectively. Deduced ATP-GTP binding sites are wavy underlined and highlighted as shaded region. (A): Amidation site of EsHSC70-5 is underlined. Three N-glycosylation sites are circled in red. cAMP- and cGMP-dependent protein kinase phosphorylation site is wavy underlined. Casein kinase II phosphorylation sites are double underlined. Leucine zipper pattern sequence is boxed and shadowed. Protein kinase C phosphorylation sites are indicated by dotted line. Tyrosine kinase phosphorylation site is highlighted as shaded region. (B): Signal peptides sequence of EsHSC70-3 is wavy underlined. Endoplasmic reticulum targeting sequence is double underlined and shadowed. Casein kinase II phosphorylation sites are highlighted as shaded regions. Protein kinase C phosphorylation sites are boxed and shadowed. Tyrosine kinase phosphorylation site is double underlined. Non-organelle consensus motif is underlined and shadowed.

Figure S2. Multiple alignment of representative HSC70-5 amino acid sequences. (A): Predicted HSP70 domain with some nucleotide-binding sites from BLASTX; (B): α helices and β -sheets of EsHSC70-5 are indicated by ESPript 3.0 (<http://esprpt.ibcp.fr/ESPript/cgi-bin/ESPript.cgi>). Three HSP70 family signatures sequences are boxed in green. See **Table S3** for GenBank accession numbers. Consensus sequences of the HSC70-5s are highlighted with red background.

Figure S3. Multiple alignment of representative HSC70-3 amino acid sequences. (A): Predicted HSP70 domain with some nucleotide-binding sites from BLASTX; (B): α helices and β -sheets of EsHSC70-3 are indicated by ESPript 3.0 (<http://esprpt.ibcp.fr/ESPript/cgi-bin/ESPript.cgi>). Signal peptides sequences are boxed in purple. Three HSP70 family signatures sequences are boxed in green. See S3 Table for GenBank accession numbers. Consensus sequences of the HSC70-3s are highlighted with red background.

Figure S4. Phylogenetic analysis of EsHSC70s and other representative HSC70s and HSP70s are inferred using

the Neighbor-Joining method. Bootstrap values greater than 50% for neighbor-joining (NJ) analysis is shown above major branches. The scale bar represents 0.02 substitutions per site. An asterisk indicates a branch having less than 50% bootstrap values support. The species names, common names and the GenBank accession numbers of all taxa are listed in [Table S2](#).

Figure S5. The predicted three-dimensional structure of EshSC70-5 and EshSC70-3 from *Eriocheir sinensis*. **(A)**. Ribbon diagram of EshSC70-5 three-dimensional structure, showing EshSC70-5 consists of two domains and possesses a distinctive α/β fold, α helices, β strands and loop are colored blue/green, yellow and red respectively. The partial enlarged view showed ATP-GTP binding site in green (nests such as GLY175, GLU176, ALA177, TYR178, LEU179, ASN180, THR181 and PRO182 are marked in purple). **(B)**: Ribbon diagram of EshSC70-3 protein 3D-structure. In the upper part, the partial enlarged view showed non-organellar consensus motif in brownish red (nests such as ARG323, ALA324, LYS325, PHE326, GLU327, GLU328 and LEU329 are shown in purple); In the lower half, the partial enlarged view showed ATP-GTP binding site in green (nests such as ALA156, GLU157, ALA158, TYR159, LEU160, GLY161, LYS162 and THR163 are shown in purple).

Table S1. The sampling number for various organs of *Eriocheir sinensis* at different larvae stages and immune challenge stress.

Table S2. Blastp homology search partial results of EshSC70-5 (A) and EshSC70-3 (B) amino acid sequence.

Table S3. Analytical procedures urls for bioinformatic analyses of EshSC70-5 and EshSC70-3 sequences.